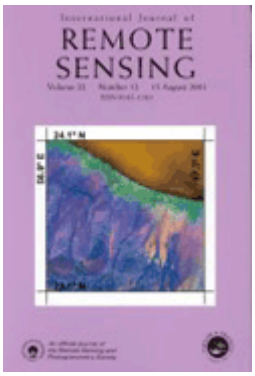

Mapping sugarcane biomass using remote sensing

Journal:	*International Journal of Remote Sensing*
Manuscript ID:	draft
Manuscript Type:	Special Issue Paper
Date Submitted by the Author:	
Complete List of Authors:	Odhiambo, Johannes; University of Nairobi, Environmental and Biosystems Engineering Wayumba, Gordon; University of Nairobi, Geospatial and Space Technology Inima, Albert; University of Nairobi, Environmental and Biosystems Engineering Omuto, Christian; University of Nairobi, Environmental and Biosystems Engineering; FAO SWALIM
Keywords:	ANALYSIS, BIOMASS, LEAF AREA INDEX, REFLECTANCE
Keywords (user defined):	ANALYSIS, BIOMASS, LEAF AREA INDEX

International Journal of Remote Sensing Vol. X, No. X, February 2009, xxx-xxx

C. Omuto and P Paron

Potentialities and limitations Issue
Taylor & Francis

Special Issue Paper

Mapping sugarcane biomass using remote sensing

ORODI ODHIAMBO*[1], GORDON WAYUMBA[2] ALBERT INIMA[1] and CHRISTIAN OMUTO[1]
1 Environmental and Biosystems Engineering Department, University of Nairobi, P.O. Box 30197-00100, Kenya
2 Geospatial and Space Technology Department
University of Nairobi, P.O. Box 30197, Nairobi
26 February 2009

* orodijo@uonbi.ac.ke

Abstract

Monitoring biophysical features of sugarcane to estimate productivity of growing cane using ground-based crop cut techniques require immense time and equipment.

Crop biophysical parameters from representative Mumias Nucleus Estate sugarcane fields were used to characterize biomass by gleaning spectral reflectance values to calculate five vegetation indices and comparing them with ground-truthed data clipped from the fields.

Results indicated leaf area index and Red/Near infrared as the best biomass predictors with Coefficients of correlation (r^2) of 0.94 while a strong relationship existed between the spectral values and field biomass with predictions of r^2 of 0.78 and 0.82 for bands 3 and 4 respectively.

Temporal maps developed using transformed values of bands 3 and 4 suggested that yield and biomass could be mapped from ETM+ satellite imagery. A model developed performed well returning a coefficient of efficiency of 0.98 confirming the potential of remote sensing in providing data to estimate crop yield.

1.0 Introduction

Monitoring biophysical features of sugarcane using remotely sensed data is crucial for many purposes, such as estimating productivity of growing and mature cane, monitoring sugarcane health and vigor and understanding sugarcane ecological processes.

In the energy sector, sugarcane biomass provides a safe, sustainable and potentially big source of energy that can augment the industrialisation process in Kenya. A sustainable biomass system forms a closed cycle of carbon increasing the importance of fuel from biomass in terms of global and regional scales.

However, effective biomass resource management for any production system depends on accurate assessment of the kind, amount, and condition of the existing biomass resources. Currently the crop cut census method used to forecast and predict sugarcane biomass production is tedious, inaccurate and time consuming calling for the development of a more appropriate methodology to ameliorate these problems. Kituyi (2001) ascertains that the temporal and spatial patterns of biomass in Kenya are not known.

This study attempted to provide part of the answer to the question of spatial and temporal variability of biomass by using rapid assessment to test the combined application of digital mapping in predicting biomass in Mumias Nucleus sugarcane fields by integrating Remote Sensing (RS) and Global Positioning Systems (GPS) techniques.

Studies have been done and point at the existence of relationships between spectral reflectance measurements and leaf area index (LAI) and total aboveground green biomass (Guo, *et al*, 2000). RS by satellites can provide relatively homogenous sample over extensive geographical areas through a range of spatial, temporal and spectral resolutions depending on the satellite (Hay *et al.*, 1997). RS can also be used to establish the statistics of the cultivated areas and the progress of the crops, to predict the harvest and to provide continuous and extremely prompt information on the state of growth of the main crops and the degree of damage caused by pests, disease and other agents, which affect the actual yield (Thiede G, 1980).

RS integrated with GPS have been found to have the capacity to provide valuable information regarding various natural resources (Skidmore, 1997 and Warren, 1990) over a wide area in a timely and cost effective manner. Parodi (2000) detailed how to determine the structural biophysical parameters of a crop using satellite imagery data. The biophysical properties that characterize sugarcane include LAI (established from the number and area of leaves) and, percent vegetation cover (%), species richness and unit area, plant biomass or total aboveground green biomass (g/m^2), canopy height (m) and plant moisture content (g/m^2) (Guo, X., *et al.*; 2000, Maas, 1998; Wiegand *et al.*,

1992).Other incidental properties include; the chlorophyll content and rate of photosynthesis, the brix, sucrose, purity and fibre content of the crop.

2.0 Methodology

2.1 *Study area*

The study was conducted in the 3,300 hectares Mumias Sugar Company Nucleus Estate in Mumias-Butere district, Kenya (Figure 1). The area was chosen since Mumias Sugar Company a major user of biomass from sugarcane for cogeneration with an installed generation capacity of 5 MW (Ministry of Energy, 1992) that is intended to be increased to 30 MW making mapping of sugarcane biomass significant. The area also lends itself well for the use of satellite imagery as it has large fields with one type of crop with the parcels grouped into economical blocks each covering at least 6 hectares ensuring homogeneity of the biophysical properties. In this area, the net earnings from sugarcane has not kept pace with inflation and economic growth putting a need to improve production while lowering costs (KSB, 2002). The study therefore, aimed at giving a rapid methodology for predictive spatial and temporary mapping of sugarcane biomass as a step towards lowering the production costs.

2.2 *Data*

2.2.1 Remote sensing image One nearly cloud-free, ETM+ image of February 22, 2003 for path 169, row 70 covering the study area was obtained from World Agro forestry Center (ICRAF) Kenya. The intention was to select a satellite image covering a period with low cloud cover and minimal constraints in conducting fieldwork**.**

2.2.2 Measurement of crop biophysical properties
Field data was collected for sugarcane at the fifteenth (field 34) and sixteenth (field 35) months of growth (Figure 1). The ages were selected to coincide with the critical sugarcane phonological stages of maturity and senescence. For each field and date, plant samples were taken and their structural parameters measured. The two sugarcane fields studied (figure 1) were of sizes 9 ha and 15 ha respectively. For each field of study, clipping was done in blocks randomly placed on a W shaped transect. Field 34 had 5 blocks while field 35 had 4 blocks. Each block was 20 m by 20 m in size to ensure that it fitted within a single ETM+ pixel (Figures 1 and 2).

The nine randomized sampling blocks were used as they meet the minimum number recommended by Congalton ((1986) i.e. number of sites should be greater than n+1, where n is the number of bands of the imagery used. In this case, n was 6). Given an error of less than one pixel in positional accuracy for the satellite imagery, an exclusion buffer of 30 m, or one pixel, was applied when extracting the at satellite reflectance pixel values for each field to reduce edge effects. From each block, four 1.5m x 1.5m sampling plots were clipped for biomass study along a cross (+) shaped transect (figures 2).

Detailed sampling was done for cane to provide biophysical (cover and spatial biomass variability, average plant height, the weight of wet and dry biomass and the leaf water content and leaf specific weight) in-situ data for correlation with spectral data (Tables 1 and 2). Nitrogen, brix and sucrose contents were also determined in the Mumias company agronomy laboratory to establish the consistency of the sugarcane crop studied. Besides, cultivation data and selected meteorological data were recorded. Accurate field boundary information for the nucleus estate farms was obtained for the 2002-2003 season. Expected sugarcane yield, fertilization, ploughing details, seeding date and density, variety, and harvest date information was obtained for these fields. The Global Positioning System (GPS) reading was obtained at the centre of each sampling plot using a hand held Garmin® 12 XL GPS unit to establish plot locations in Kenyan Universal Transverse Mercator (UTM) coordinates. The geographic location of each sample site was recorded within a positional accuracy of 0.15 pixels or 4.5 m.

2.2.3 Analysis The ETM+ image for February 2003 was geo-referenced and corrected for geometric error by first transforming the February image to the UTM projection in zone 36. The

geometric transformation equation was computed using six-ground control GPS acquired coordinates that produced a final root mean square (RMS) error of 0.15 pixels. This error was less than 0.35 pixels recommended for ecological studies. The image was then registered to two 1:50 000 normal scale digital topographical sheets (GoK, 1971) covering Mumias Sugar fields. Atmospheric correction was done according to the method described by Chavez (1996).

Spectral values extracted from the acquired ETM+ February 22, 2003 image were transformed into Vegetative Indices (NDVI, SAVI, R/NIR, R/MIR and NIR/MIR) using ILWIS™ software. The spectral values were also used to derive biophysical parameters (f-PAR, f-Cover and LAI, and Accumulated Biomass) at the sampling points using a script written and run in ILWIS™ (ILWIS, 2005). The extracted spectral values and the transformed indices and biophysical parameters are listed in tables 2 and 3 for field 34 and 35 respectively.

Pearson's Correlation analysis was used to determine the linear relationships between the estimated biophysical parameters (X) and measured biomass (Y). Pearson's Correlation Coefficient measures the strength of the linear relationship between two variables. The statistical significance of *r* was tested using a t-test. The correlation coefficient r (also called Pearson's product moment correlation) was calculated using equation (1).

$$r = \frac{\sum_{i=1}^{n}\left(x_i - \bar{x}\right)\left(y_i - \bar{y}\right)}{\sqrt{\sum_{i=1}^{n}\left(x_i - \bar{x}\right)^2 \sum_{i=1}^{n}\left(y_i - \bar{y}\right)^2}} \quad \ldots\ldots\ldots\ldots\ldots\ldots 1$$

Calibration of biomass productivity classes with remote sensing data Pearson's Correlation analysis was used to determine the linear relationships between the estimated biophysical parameters (X) and measured biomass (Y). Pearson's Correlation Coefficient measures the strength of the linear relationship between two variables. The statistical significance of *r* was tested using a t-test. The correlation coefficient r (also called Pearson's product moment correlation) was calculated using equation (1).

ArcView 3.2a, ERDAS 8.4 Imagine and ILWIS software were used in an integrated manner to map and to resize maps and allocate points in the study area. Mapping of biomass in dry weight was based on predicted biomass yield of sugarcane at the age of 16 months using information derived from the ILWIS output. Mapping was done to provide a visual picture of the integration of interaction of factors affecting biomass yield distribution.

3.0 Results and Discussions

Field 35 was sampled when at senescence stage while field 34 was sampled at an active growing stage. Field 34 had higher chlorophyll content than field 35 and therefore showed the brighter red colour than that of field 35 (Figure 3). Among the transformed datasets, R/NIR was the best vegetative index for predicting biomass at senescence stage while NDVI was a better predictor at the crop growing stage (Figure 4).

For biophysical parameters, LAI was the best predictor of biomass at both crop senescence and growing stages (figure 4). However all biophysical parameters and band 4 were negatively correlated with measured biomass at senescence and positively correlated at crop growing stage (Figures 4 to 8).

At senescence stage (field 35, figure 4), most of the crop biophysical properties (LAI, f-cover, greenness etc) diminish while biomass increases until it reaches a maximum value. At the crop growing stage (field 34, figures 7 and 8), the increase in the biophysical properties of the crop signifies continued crop development with an attendant biomass accumulation. This accounts for the positive correlation at the growing stage.

There was a strong relationship between biomass and most spectral variables. The ETM+ visible bands were consistently the most strongly correlated with biomass, with band 1(blue-green), band 3, and band 4 (near infra-red) being the stronger predictors (r^2 = 0.93,0.85, and 0.91, respectively). Band

6 was also found to be a good predictor of biomass (r^2=0.86) (Figures 5 and 6). This corroborates the works of Todd *et al*. (1998) who found band 3 to be the best predictor of biomass for the steppes of eastern Colorado.

The predictions were improved further when the analysis was done pixel-by-pixel giving the best prediction of r^2 of 0.98 (Figure 5). In comparison, when the sample points where averaged to cover half a pixel, the prediction was slightly lower (r^2 =0.92). The lowest prediction was given when the point were considered point by point (r^2 = 0.81) (Figure 6).

A comparison between the observations taken at different image acquisition dates indicates better results for data gleaned closer to satellite overpass date than that gleaned nearly a month later (Figure 6 and Figure 7). This confirmed the importance of temporal resolution in remote sensing as it limits its application to the period of data acquisition (Millinton and Townseed, 1989, Lillesand and Kiefer, 2000).

3.1 *Prediction Model*

From regression analysis, a yield mapping model was developed for estimating biomass yield in t/ha for a sugar cane crop at senescence stage. This was done using the best biophysical parameter computed by transforming spectral values. The model developed was derived as;

$$Accbiomass = Estbiomass * k - c \qquad 2$$

Where; Accbiomass is the predicted biomass in t/ha
Estbioms is the estimated biomass calculated as;

$$Estbioms = \sum_{i=1}^{n} s(t) * AcAPAi$$

k and c are constants derived as 1.017 and 13.7 for Mumias Nucleus Estate

A script written using the developed model was then run in ILWIS to map biomass using the February 2003 ETM+ image clipped to cover the Mumias Nucleus Estate. The map in figure 9 is the biomass prediction map of the Estate showing three levels of production; high (blue), medium (green) and sparse (brownish).

The script determines the crop biophysical properties like LAI, f-PAR, f-cover, NDVI and SAVI and uses the methodology developed by Liang (2004) to estimate and map biomass based on energy fluxes derived from radiation indices extracted from the image.

3.2 *Model validation*

The model validation was conducted by comparing the in-situ measurements and the derived biomass parameter values (figure 10). The comparisons of crop structure parameters showed a high coefficient of correlation (r2) of 0.98 for analysis done pixel by pixel (Blocked). This was repeated for half the block in which case two samples were averaged from each block. The half block comparisons gave a lower correlation value (r^2 of 0.92).

Finally, comparisons were made point by point that gave the lowest correlation value (r^2 of 0.81). The student t test returned a higher r^2 value of 0.92 for block analysis compared to r^2 of 0.82 for point-to-point analysis.

3.3 *Errors and contingencies*

All predictions show an absolute value for ARPE of no more than 0.02%. The ARPE values (-0.0175 and 0.0175) for the validation data sets indicate a highly satisfactory performance of the model. The SSE was 19 for the pixel-by-pixel analysis with a C_{eff} value of 0.98 showing excellent predictive ability.

In general, better or comparable predictive ability of models were obtained for most of the parameters, compared to previously reported values in the literature.

For example, in a recent study, Thenkabail *et al*. (2000), in their experiment based on a spectral data set acquired from a hand-held spectroradiometer, obtained significant r^2 values for four-TM models of 0.78, for LAI.

In this study, a value of 0.81-0.99 was found. For the NDVI-based models, the 0.86 got is less than in this study case that gave the highest r^2 value of 0.93. Shanahan *et al*. (2001) reported significant r^2 of about 0.9 between corn yield and broadband NDVI. They acquired images from an airborne platform in four TMs over an experiment with varying nitrogen levels. Similarly, in an experiment over different corn hybrids grown under various nitrogen levels, Blackmer *et al*. (1996), using a portable spectroradiometer, reported r^2 values for yield prediction models ranging between 0.70 and 0.99.

4.0 Conclusions

The study shows that ETM+ crop reflectance can be used to predict biomass yields in sugarcane fields. Mature sugarcane biophysical parameters were well predicted in spectral reflectance. Yield forecast results from the reported study show that sugarcane yields can be predicted from single-date ETM+ crop reflectance.

The results remained positive for comparisons across the field for predicted values and measures mature sugarcane field. In general, a good agreement between the observed and predicted values of various parameters was observed. When the VI-based models for estimating biomass measurements were compared to the single reflectance TM-based models, the former were found to be better, thus making a case for the use of VI-based models.

5.0 Acknowledgement

We thank Mr. Patrick Chebosi and the Mumias Sugar Company crew for helping with the field and laboratory work. To them, we owe much for the costs incurred to facilitate this work.

Appendices

See attached files on figures and tables

References

Betrann MC, and Belmonte AC, 2001. Irrigated crop area estimation using LANDSATimagery in La Mancha Spain, *Journal of Photogrametric Engineering and remote sensing*, American society of Photogrammetry and remote sensing, Vol 67(10), pp1177-1184.

Blackmer TM and Schepers JS. 1996. Aerial photography to detect nitrogen stress in corn. Journal of. Plant Physiology. 148:440–444.

Chavez PS, 1996, Image based atmospheric correction-revisted and improved, *Photogrammetric Engineering and Remote Sensing*, 62(9), 1025-1036

Congalton RG, 1986, Accuracy assessment and validation of remotely sensed and other spatial information, *International Journal of Wildland Fire*, Volume 10 (Issue 4) Pages 321-328 22

Congalton, **RG, Balogh MC, Bell K Green JA**, 1998, Mapping and monitoring agricultural crops and other land cover in the Lower Colorado River Basin, *Photogrammetric Engineering and remote sensing*,

GARMIN, 1998. GPS 12XL, Personal Navigator, Owners manual and Reference, Garmin (Europe) Ltd.

Government of Kenya (GoK*),* 1971, Toposheet 102.2

Guo, X., Price KP and Stiles. **JM.** 2000. Modeling Biophysical Factors for Grasslands Using LANDSATTM Data in Eastern Kansas, Annual Meeting, *The Second International Conference*

on Geospatial Information in Agriculture and Forestry. Lake Buena Vista, Florida. January 10-12.

Hall, FG, Shimabukuro, Y.E, Huemmrich, K.F, 1995, Ecological Applications, Remote Sensing of Forest Biophysical Structure Using Mixture Decomposition and Geometric Reflectance Models. Forrest

Hay S, Rogers JD, Wint WGR. Natural Resource Assessment for Nigeria: *Using Meteorological satellite data to map land cover*, Technical Applications, pp 23.

ILWIS 3.2 academic, 2005, ITC, The Netherlands

International Centre for Research in Agro forestry, ICRAF, (2000). Improved Land Management in the Lake Victoria Basin: Linking Land and Lake, Research and Extension, Catchment and Lake Basin*, Final Technical Report, start-up phase July 1999 to June 2000, pp 1.*

Kituyi E, Marufu,L,Huber,B, Wandiga, S.O, Jumba S.O, Andreae, M.O, Helas, G 2001. Biofuel consumption rates and patterns in Kenya, *Biomass and Bio energy Journal*, Pergamon.

Kituyi, E, Marufu,L, Wandiga, S.O, Jumba S.O, Andreae, M.O, Helas, G 2001. Biofuel Availability and domestic use patterns in Kenya, *Biomass and Bio energy Journal*, Pergamon.

Liang,S, 2004, Quantitativ remote sensing of land surfaces (New Jersey), John Wiley and Sons.

Lillesand TM, and Kiefer RW, 2000. Remote sensing and image interpretation 4th Edition, John Wiley and Sons inc. USA. 23

Malingreau JP. 1989. Vegetation index and the study of vegetation dynamics, Proceedings of a course held by the joint research centre of the commission of European Communities in the framework of the ISPRA-courses, Italy pp 285-301.

Matsuda, S, Kubota, H and Iwaki H. 1982 Biomass energy: Its possibility and limitation. *Science* 52: 735-741.

Millington A and Townseed 1989. Biomass Assessment, Woody biomass in the SADCC region.

Ministry of Energy 1992**.** Government of Kenya, Survey on Recurrent and Renewable Energy Systems for Rural Development in Kenya.

Omuto CT, 2003. Rapid mapping of hydraulic conductivity in a tropical watershed. MSc (Agricultural Engineering) Thesis. University of Nairobi.

Parodi Ir G., 2000. AVHRR Hydrological Analysis System – Algorithms and theory, Version 1.0. WRES, ITC, The Netherlands

Skidmore,A.K, Bijker,W, Schmidt K, Kumar L 1997. Use of Remote Sensing and GIS for Sustainable land management, *ITC Journal*, pp 302

Thenkabail, PS., Smith RB., and Paw ED. 2000. Hyperspectral vegetation indices and their relationships with agricultural crop characteristics. *Remote Sensing of Environment.* 71(2): 158-182.

Van der Kwast J and Zomer R. 2002. Land cover classification and DEM generation using SPOT and LANDSATimages in the lake Victoria Basin, Western Kenya, ICRAF and Universitiet Ultretch, Netherlands.

Wiegand, CL, Richardson AJ and Nixon RJN. 1992. Spectral component analysis: A bridge between spectral observations and agrometeorological crop models. *IEEE Trans. Geoscience and Remote* -24: 83-88.

.

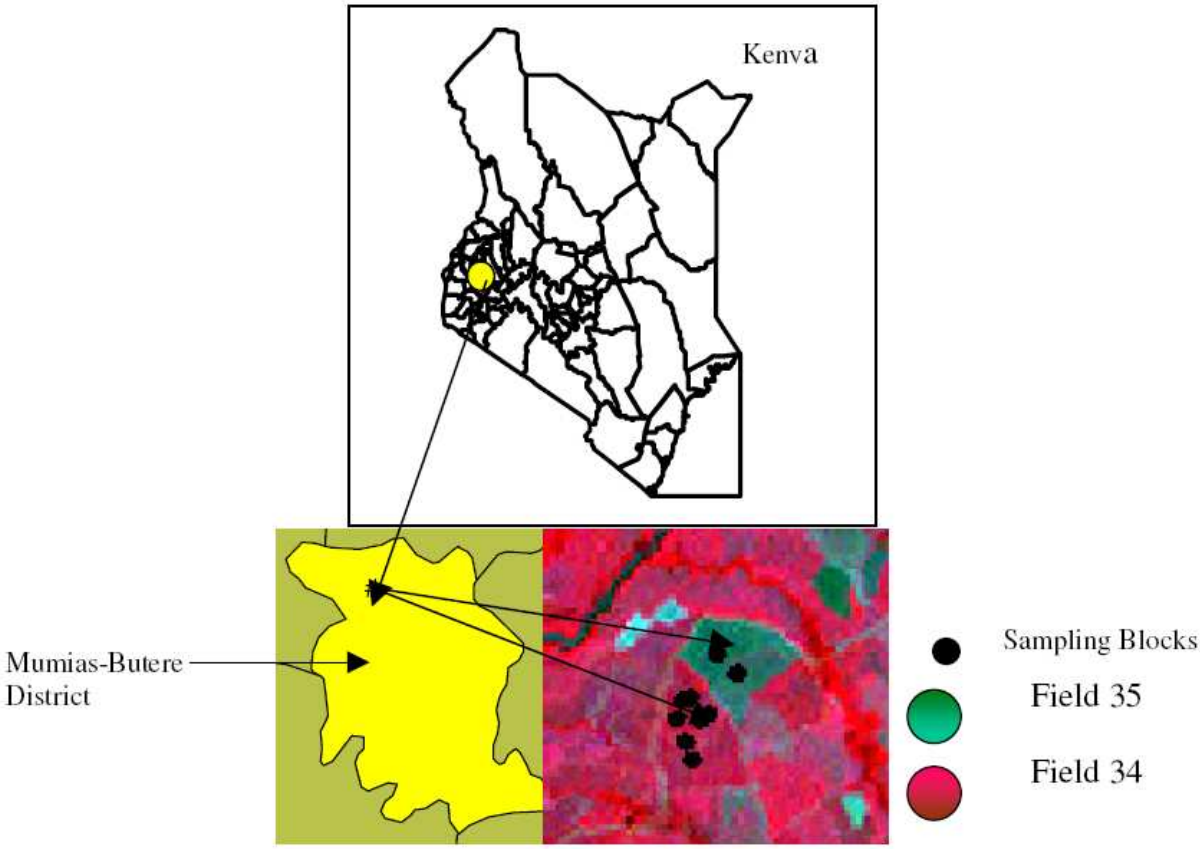

Figure 1: Study Area and Fields

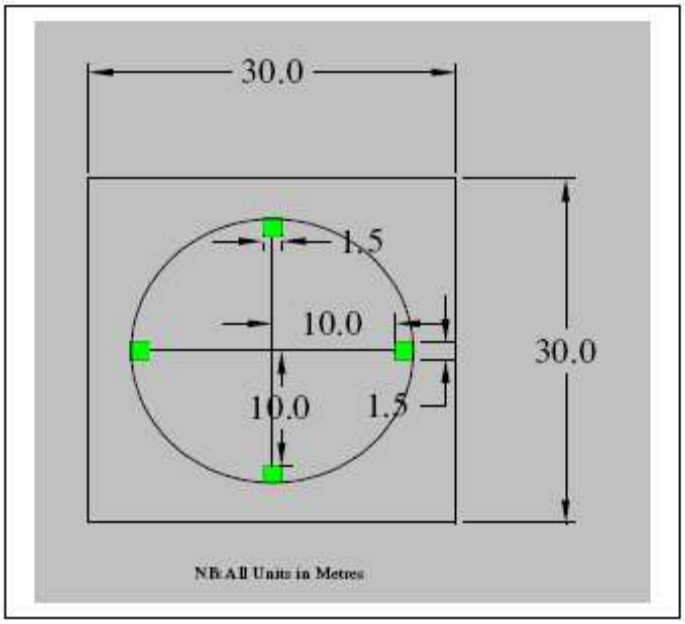

Figure 2: Layout of Clipping Plots in a Block

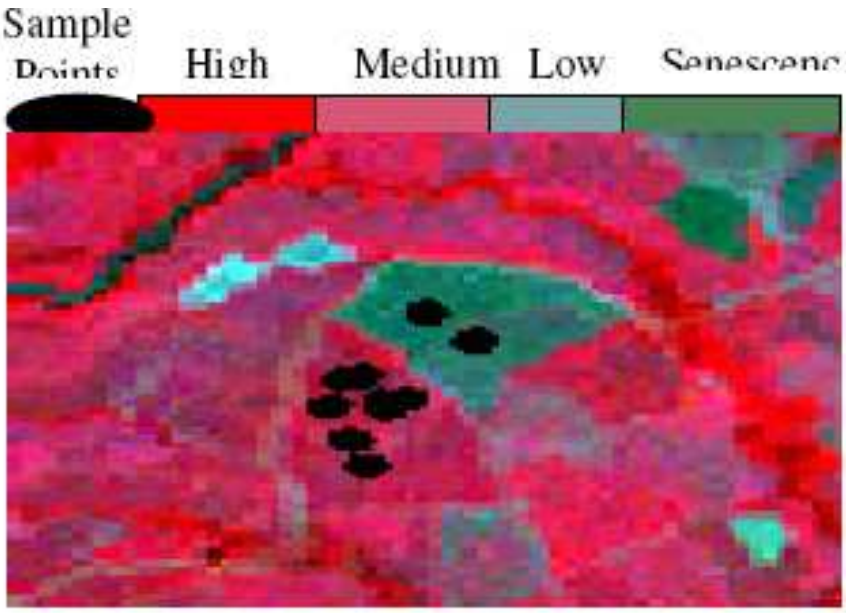

Figure 3: Fields 34 and 35

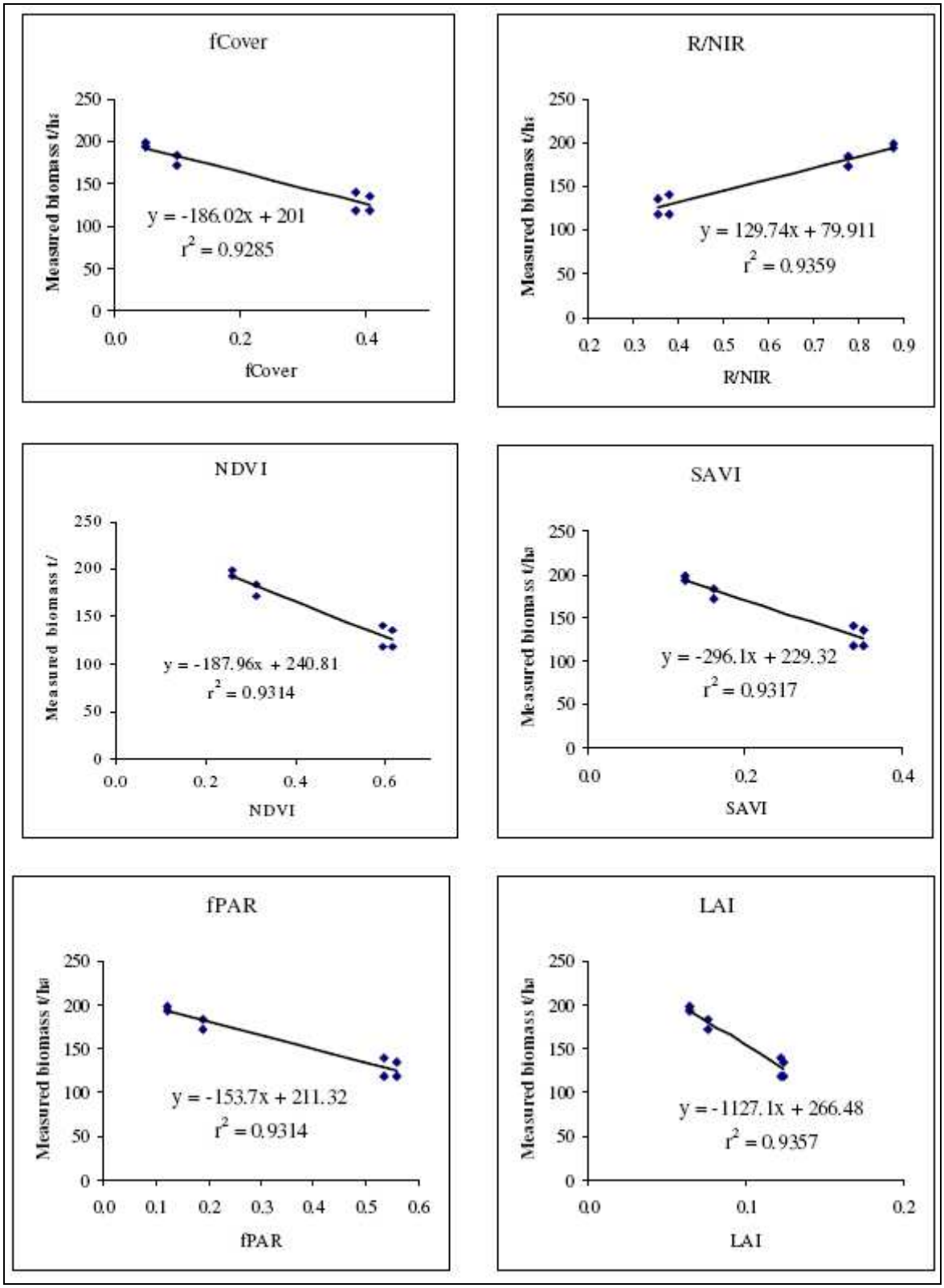

Figure 4: Biophysical vs measured biomass pixel by pixel (field 35)

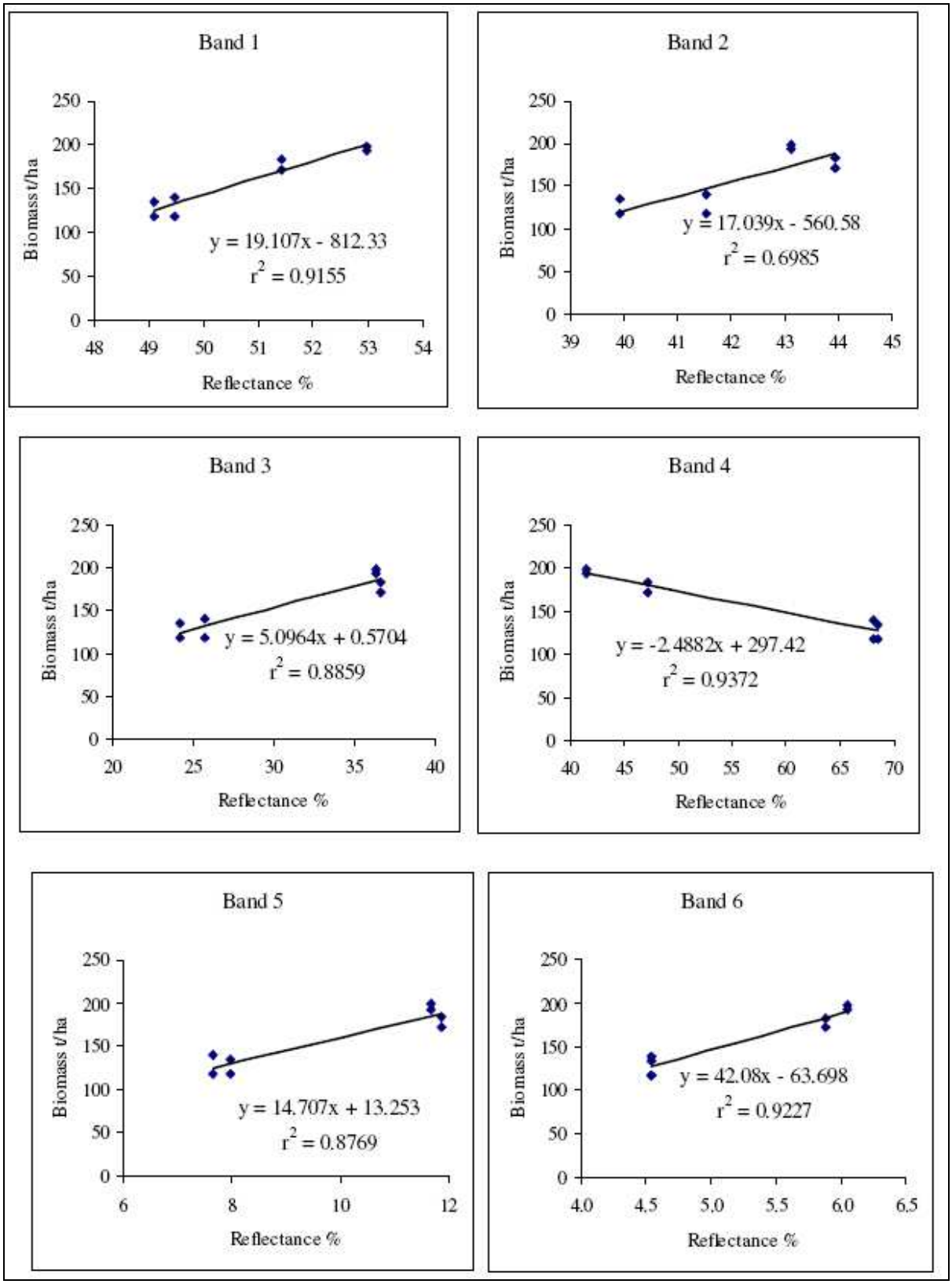

Figure 5: ETM+ reflectance vs measured biomass (pixel by pixel) on field 35

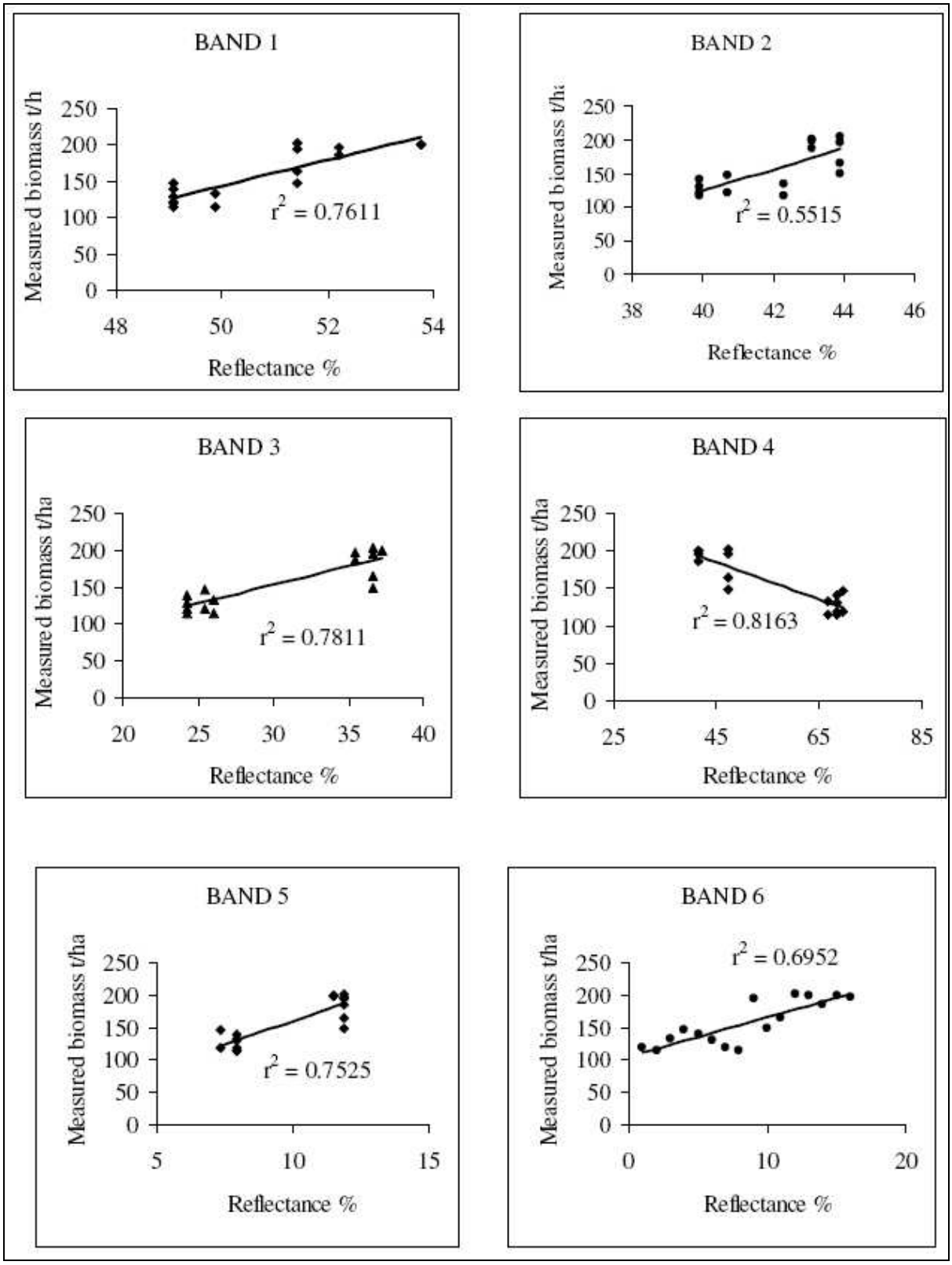

Figure 6: ETM+ reflectance vs. measured biomass on all sampling points (field 35)

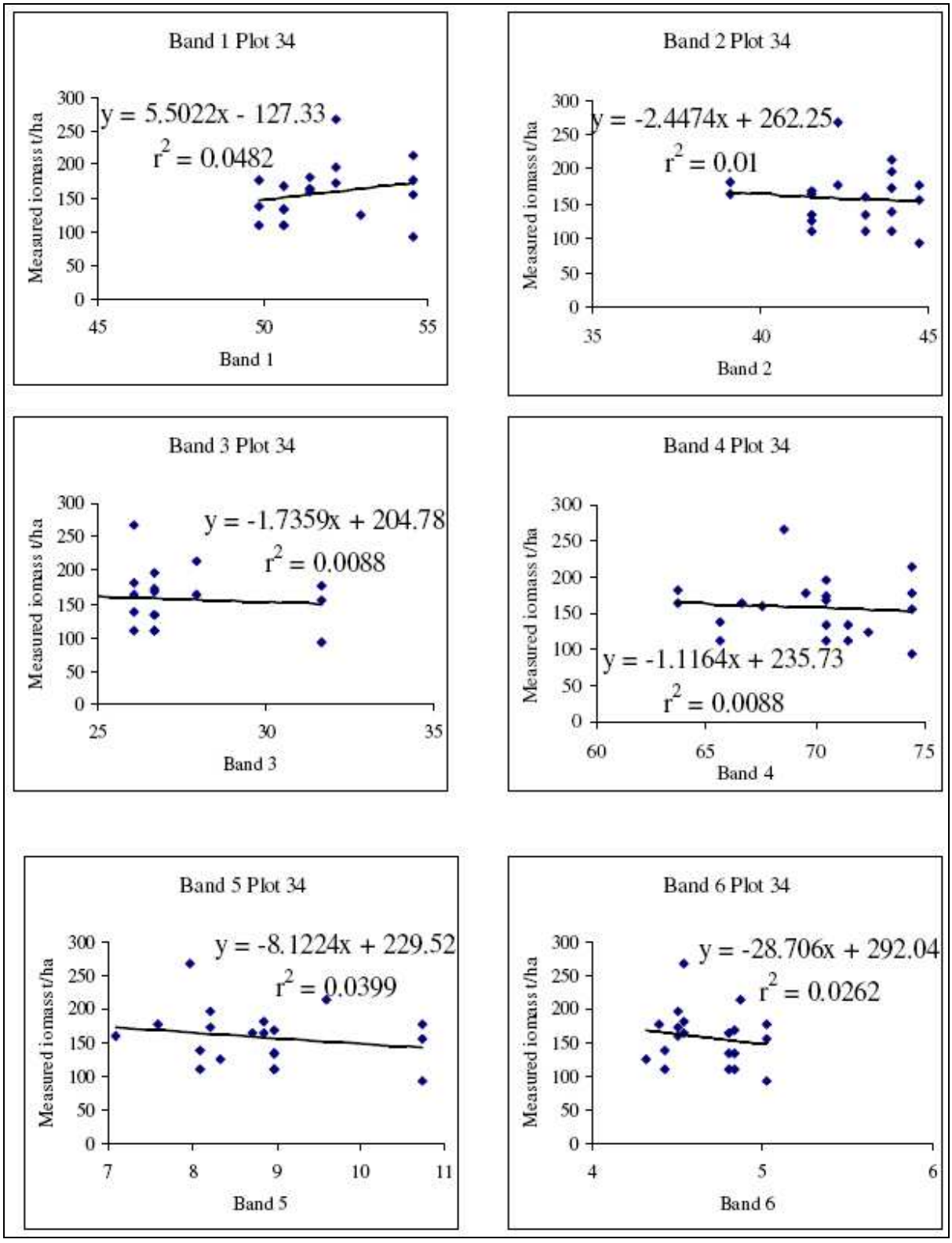

Figure 7: TM reflectance vs. measured biomass for all sampling points (field 34)

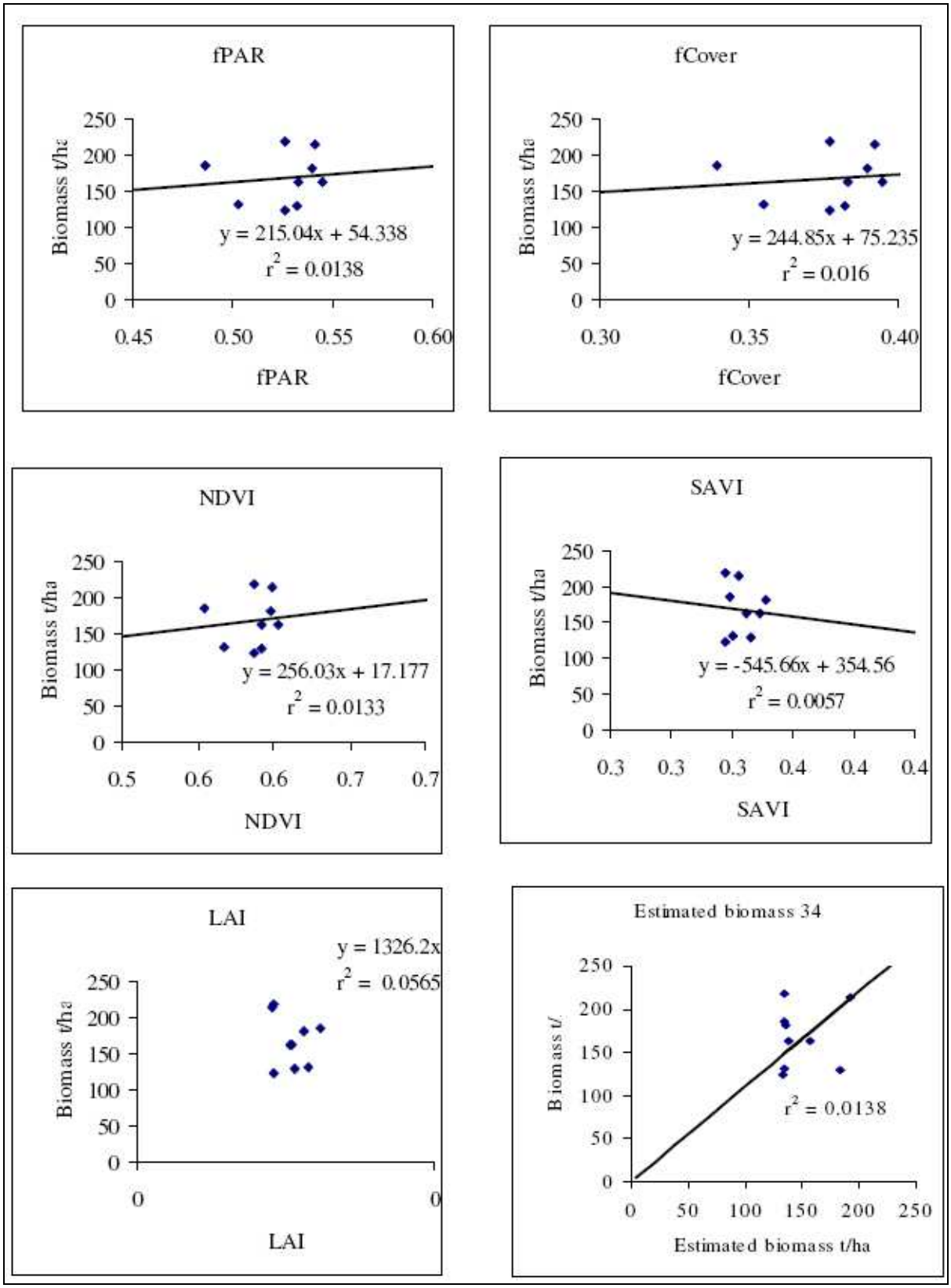

Figure 8: Biophysical vs measured biomass bi-pixel by bi-pixel (field 34)

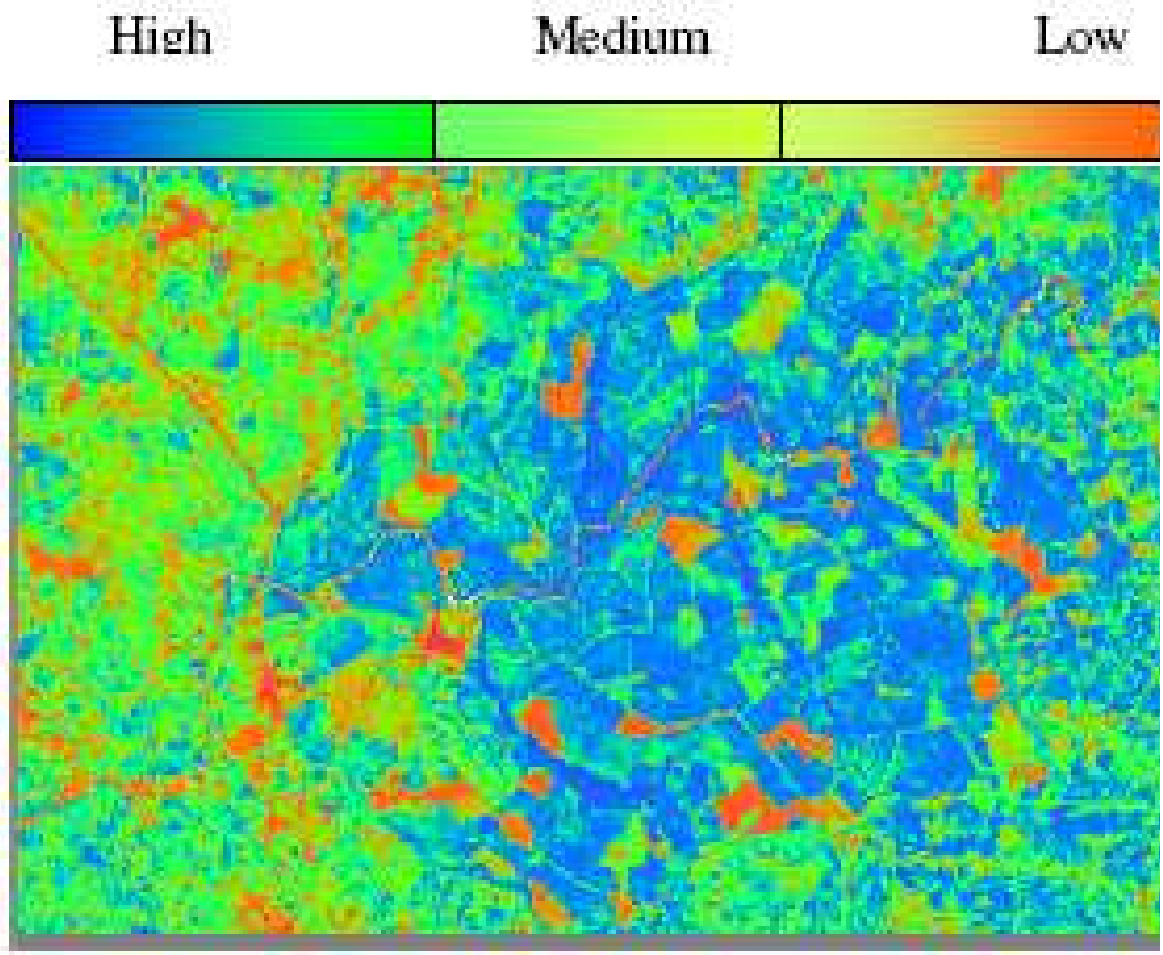

Figure 9: Map output of Mumias sugarcane

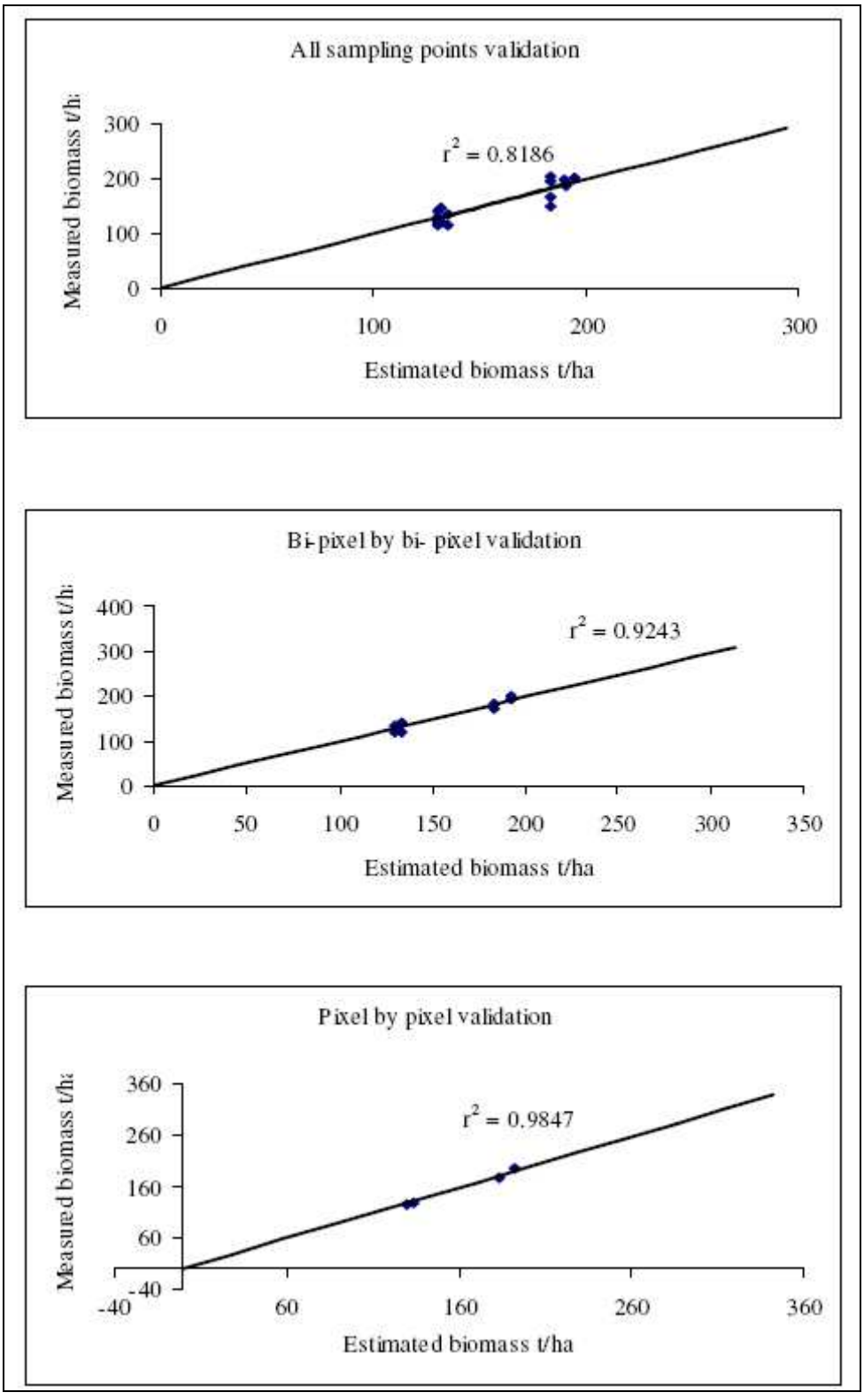

Figure 10: Validation; Estimated vs measured data

Table 1: Clipped Biomass Data

Field 34					
Block No.	Plot No.	Biomass t/ha	Block No.	Plot No.	Biomass t/ha
1	41	196	3	61	133
	42	213		62	138
	43	178		63	111
	44	173		64	111
2	51	160	4	71	267
	52	156		72	111
	53	178		73	133
	54	93		74	169
5	81	164	5	83	164
	82	124		84	182
Plot 35					
Block No.	Plot No	Biomass t/ha	Block	Plot No	Biomass t/ha
1	11	120	3	31	196
	12	116		32	148
	13	133		33	164
	14	147		34	203
2	21	222	4	41	200
	22	130		42	187
	23	120		43	200
	24	116		44	240

Table 2: Spectral values for biophysical features for field 34

	Estimated biophysical Parameters											Biomass t/ha	
Plot	fPAR	B1	B2	B3	B4	B5	B6	fCover	NDVI	SAVI	LAI	Measured	Estimated
B3411	0.53	52.21	43.93	26.70	70.51	8.21	4.50	0.38	0.59	0.35	0.13	196	134.026
B3412	0.54	54.54	43.93	27.95	74.38	9.60	4.87	0.39	0.6	0.36	0.13	213	133.499
B3413	0.56	49.87	42.33	24.84	69.54	7.58	4.39	0.41	0.61	0.35	0.13	178	130.337
B3414	0.53	52.21	43.93	26.70	70.51	8.21	4.50	0.38	0.59	0.35	0.13	173	134.026
B3421	0.55	51.43	43.13	24.22	67.60	7.08	4.50	0.4	0.61	0.34	0.12	160	131.039
B3422	0.49	54.54	44.72	31.68	74.38	10.74	5.02	0.34	0.55	0.34	0.13	156	140.701
B3423	0.49	54.54	44.72	31.68	74.38	10.74	5.02	0.34	0.55	0.34	0.13	178	140.701
B3424	0.49	54.54	44.72	31.68	74.38	10.74	5.02	0.34	0.55	0.34	0.13	93	140.701
B3431	0.54	50.65	43.13	26.70	71.47	8.97	4.80	0.39	0.6	0.35	0.13	133	133.323
B3432	0.52	49.87	43.93	26.08	65.66	8.09	4.43	0.37	0.58	0.33	0.12	138	136.309
B3433	0.52	49.87	43.93	26.08	65.66	8.09	4.43	0.37	0.58	0.33	0.12	111	136.309
B3434	0.54	50.65	43.13	26.70	71.47	8.97	4.80	0.39	0.6	0.35	0.13	111	133.323
B3441	0.54	52.21	42.33	26.08	68.57	7.96	4.54	0.39	0.59	0.34	0.12	267	133.674
B3442	0.53	50.65	41.53	26.70	70.51	8.97	4.84	0.38	0.59	0.35	0.13	111	134.026
B3443	0.53	50.65	41.53	26.70	70.51	8.97	4.84	0.38	0.59	0.35	0.13	133	134.026
B3444	0.53	50.65	41.53	26.70	70.51	8.97	4.84	0.38	0.59	0.35	0.13	169	134.026
B3451	0.50	51.43	39.13	26.08	63.72	8.85	4.54	0.36	0.57	0.31	0.11	164	138.242
B3452	0.58	52.98	41.53	24.22	72.44	8.34	4.32	0.43	0.63	0.37	0.13	124	127.175
B3453	0.49	51.43	41.53	27.95	66.63	8.72	4.80	0.34	0.56	0.32	0.12	164	139.998
B3454	0.50	51.43	39.13	26.08	63.72	8.85	4.54	0.36	0.57	0.31	0.11	182	138.242

Table 3: Spectral values of biophysical features in field 35

Plot	Extracted spectral and biophysical parameters from LANDSAT image									Measured In-situ Values			
	B1	B2	B3	B4	B5	B6	f-Cover	NDVI	SAVI	Estimated Biomass t/ha		Measured Biomass t/ha	
										All plots	Normalized	All plots	Normalized
B3512	49.1	40.7	25.5	69.5	7.3	4.5	0.4	0.6	0.3	132	134	120	118.
B3513	49.9	42.3	26.1	66.6	8.0	4.6	0.4	0.6	0.3	135		116	
B3514	49.9	42.3	26.1	66.6	8.0	4.6	0.4	0.6	0.3	135	134	133	140
B3521	49.1	40.7	25.5	69.5	7.3	4.5	0.4	0.6	0.3	132		147	
B3522	49.1	39.9	24.2	68.6	8.0	4.5	0.4	0.6	0.4	130	130	140	135
B3523	49.1	39.9	24.2	68.6	8.0	4.5	0.4	0.6	0.4	130		130	
B3524	49.1	39.9	24.2	68.6	8.0	4.5	0.4	0.6	0.4	130	130	120	118
B3531	49.1	39.9	24.2	68.6	8.0	4.5	0.4	0.6	0.4	130		116	
B3532	51.4	43.9	36.7	47.2	11.9	5.9	0.1	0.3	0.2	183	183	196	177
B3533	51.4	43.9	36.7	47.2	11.9	5.9	0.1	0.3	0.2	183		148	
B3534	51.4	43.9	36.7	47.2	11.9	5.9	0.1	0.3	0.2	183	183	164	183.5
B3541	51.4	43.9	36.7	47.2	11.9	5.9	0.1	0.3	0.2	183		203	
B3542	53.8	43.1	37.3	41.4	11.5	6.0	0.0	0.2	0.1	195	193	200	193.5
B3543	52.2	43.1	35.4	41.4	11.9	6.1	0.1	0.3	0.1	191		187	
B3544	53.8	43.1	37.3	41.4	11.5	6.0	0.0	0.2	0.1	195	193	200	200.